ТЕХНІКА ТА МЕТОДИ ЕКСПЕРИМЕНТУ
ENGINEERING AND METHODS OF EXPERIMENT

УДК 621.384.6+615.849 https://doi.org/10.15407/jnpae2020.02.200

Mohamed Bencheikh[1,*], Abdelmajid Maghnouj[2], Jaouad Tajmouati[2]

[1] *Physics Department, Faculty of Sciences and Technologies Mohammedia, Hassan II University of Casablanca, Mohammedia, Morocco*
[2] *LISTA Laboratory, Physics Department, Faculty of Sciences Dhar El-Mahraz, University of Sidi Mohamed Ben Abdellah, Fez, Morocco*

*Corresponding author: bc.mohamed@gmail.com

ANALYSIS AND EVALUATION OF SECONDARY PHOTONS ORIGINATED IN JAWS AS CONTAMINATION PARTICLES AT THE PHANTOM SURFACE

The present work is focused on the study of the geometry and material of a beam modifier (jaws), which is crucial for Linac improvement by reducing secondary photons emergent from it. They have negative effects when the cancer was treated and especially in the deep tumor because their energy is deposited in shallower depth and could destroy the healthy cells that surround the treatment volume. The purpose of this study is to investigate and evaluate the characterizations of secondary photons originated in jaws in terms of fluence profile, energy fluence profile, energy fluence distribution, spectral distribution, and angular spread distribution. This work was performed by using the BEAMnrc Monte Carlo and BEAMDP codes. The jaws are a potential source of secondary photons nearest to the phantom. The number of secondary photons emergent from X-jaw (in-plan jaw) is higher and they are more energetic in comparison to secondary photons of Y-jaw (cross-plan jaw). Therefore, the most significant result is on the angular spread distribution of secondary photons for each pair jaw. For Y-jaw, the majority of photons are scattered and spread with high angle degree that means these photons can fall out of the irradiation field and affect the healthy cells but for the X-jaw, most of the secondary photons are within the irradiation field and they can affect healthy cells mainly only at the entrance of treatment volume.

Keywords: secondary collimator, Monte Carlo simulation, secondary photons, BEAMnrc code, BEAMDP code.

1. Introduction

In radiotherapy, the photons are produced from the target and they do not all reach the tumor treatment volume; some of them interact with the head component material and produce other particles: scattered photons (secondary photons), electron contamination etc. On the phantom surface, the beam is composed of primary photons, secondary photons, and other particles. In this study, the secondary photons, emergent from the jaws or secondary collimator, are examined and analyzed at the phantom surface.

The jaws are used to define and limit the irradiation field as a rectangular field. In this work, the irradiation field is square centered on the beam central axis. Jaws are formed by two pairs' jaw: X-pair jaw (in-plan jaw) and Y-pair jaw (cross-plan jaw). The X-pair is closer to the target but Y-pair is closer to the phantom. The characterizations of secondary photons are evaluated in terms of the fluence profile, energy fluence profile and distribution, spectral distribution, and angular distribution.

This study was carried out by using BEAMnrc Monte Carlo and BEAMDP codes. The knowledge of the characterizations of secondary photons is essential for photon dosimetry improvement and jaws enhancement in Linac development and also for the dose determination in radiotherapy treatment.

Monte Carlo simulation is a technique that provides both accurate and detailed energetic and dosimetric calculations of medical linear accelerator head, the Monte Carlo methods have been used extensively in medical physics for modeling linear accelerators and for radiation therapy dose calculation [1 - 4].

In this study, the secondary photons are investigated and analyzed for X-jaw and Y-jaw separately to displaying the radioprotection problems related to jaws because they are the last beam modifier in the photons path and the nearest Linac component to patients. The Monte Carlo geometry was built for Varian Clinac 2100 by BEAMnrc code [5]. The Linac head was modeled as realistically as possible and the simulation validation was done in our previous study [6]. The photon beam energy was 6 MV, the field size was 10×10 cm^2 and the source-to-surface distance (SSD) was 100 cm. The physical process simulation was performed based on the EGSnrc code where the transport of radiation was simulated as realistically as possible [7].

2. Materials and methods

2.1. Monte Carlo simulation

The Monte Carlo simulation was performed for 6 MV photon beam that has been produced by Varian Clinac 2100. The Linac head was simulated based on

© Mohamed Bencheikh, Abdelmajid Maghnouj, Jaouad Tajmouati, 2020

manufacturer-provided data (Varian Medical System) by BEAMnrc code. The simulation statistical uncertainty is under 1 % and this result agrees with the work of Aljamal [8]. The Monte Carlo simulation of Linac head was validated by using the gamma index method with criteria of 3 % for dose deviation (DD) and 3 mm for distance to agreement (DTA). The simulation validation is ensured by the gamma index acceptance rate of 99 % for percentage depth dose (PDD) and of 98 % for beam dose profiles [6].

After their parameters have been extracted using the BEAMDP, the secondary photons are analyzed and evaluated in terms of the fluence profile, energy fluence profile and distribution, spectral distribution and angular distribution at the phantom surface where SSD was 100 cm [9]. Fig. 1 shows the position of the scoring plane at the water phantom surface and the position of jaws in Linac head.

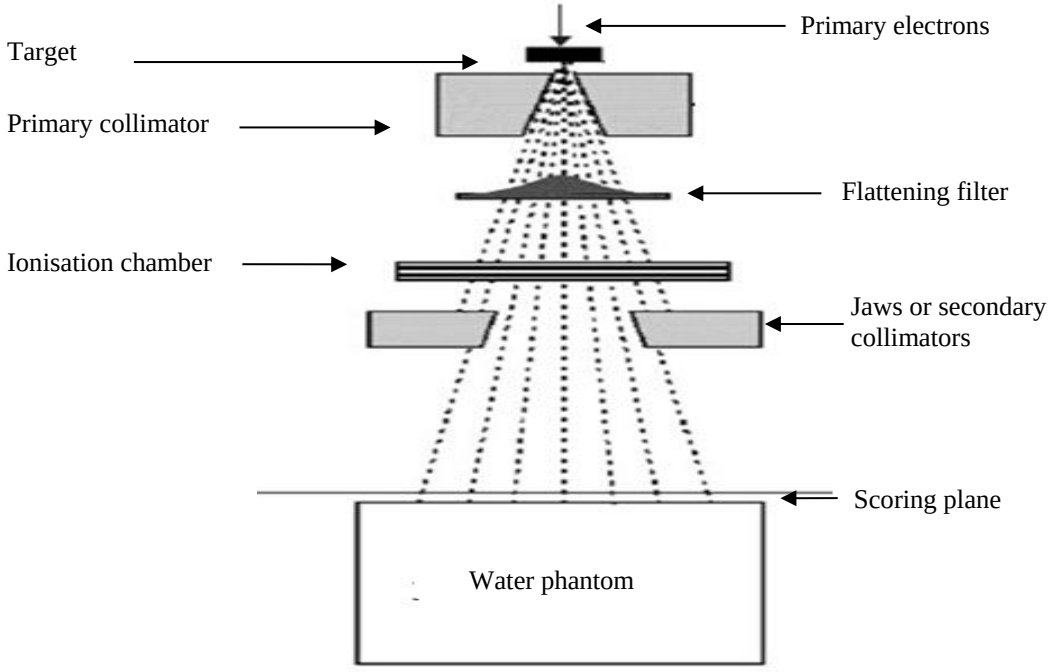

Fig. 1. Cross-section view of Monte Carlo geometry of Linac head and the position of jaws and scoring plane for phase space file at water phantom surface.

Fig. 1 shows a cross-section view of Linac head displaying the position of X-jaw and Y-jaw. The characterizations of secondary photons originated in jaws are evaluated in terms of fluence profile, energy fluence profile, energy fluence distribution, spectral distribution, and angular spread distribution.

2.2. Secondary photons characterization evaluation

The secondary photons alter the beam dosimetry at a shallower depth, and they can destroy the healthy cells at the entrance of the beam for deep tumor treatment. They have also many problems in radioprotection if their directions go out of the irradiation field. To quantify the comparison between X-jaw and Y-jaw in the production of secondary photons and their characterizations at the phantom surface, the fractional contribution (FC) of each pair jaw in all secondary photons of jaws together (total secondary photons emergent from jaws together) was evaluated for each physics characterization of the photons. It was evaluated in percentage and determined according to the formula

$$FC(\%) = 100 \cdot \frac{X_{\text{of one jaw}}}{X_{\text{of jaws together}}}, \qquad (1)$$

where FC is a fractional contribution, X is fluence profile, energy fluence profile, energy fluence distribution, spectral distribution, mean energy distribution, and angular distribution.

3. Results and discussion

3.1. Fluence profile

The fluence profile describes the variation of the number of photons as a function of off-axis distance. Fig. 2 gives the planar photon fluence profiles as a function of off-axis distance for X-jaw and Y-jaw.

It can be seen from Fig. 2, the number of secondary photons originated in jaws changed from X-jaw to Y-jaw: The X-jaw produced more secondary photons than the Y-jaw. The secondary photons production depends on the position of the jaw referring to the target. The number of secondary photons emergent from jaws together decreased with off-axis distance.

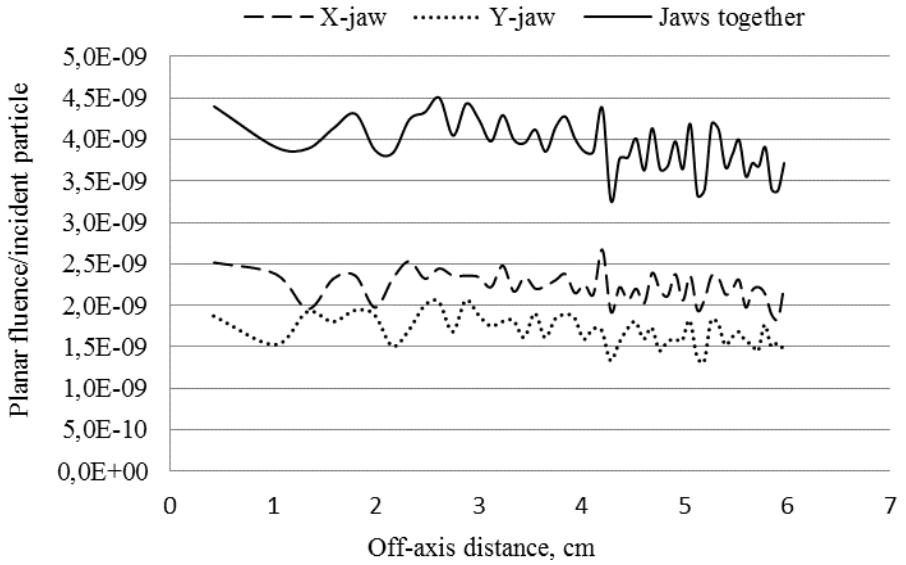

Fig. 2. Fluence profile of secondary photons originated in X-jaw and Y-jaw and jaws together as a function of off-axis distance.

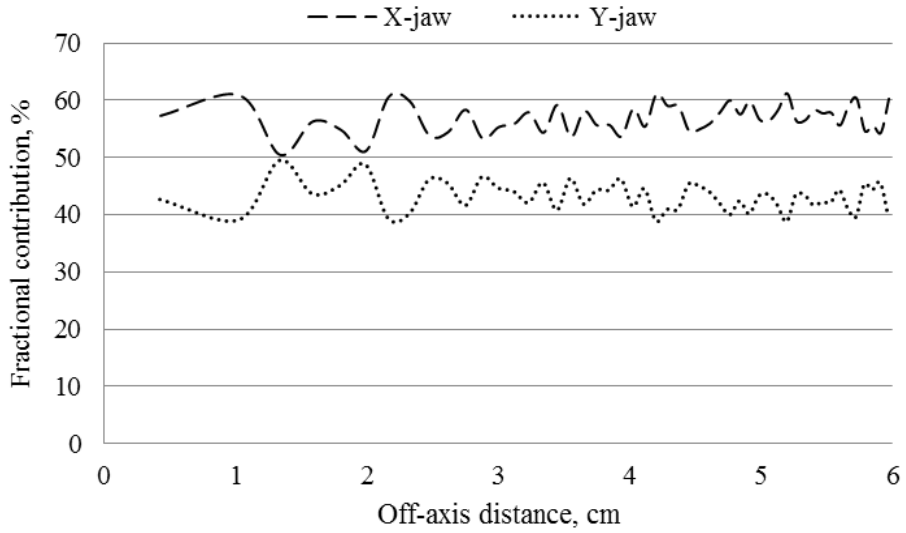

Fig. 3. Fractional contribution of photons fluence of X-jaw and Y-jaw in the fluence of jaws together as a function of off-axis distance.

Fig. 3 shows the fractional contribution of X-jaw and Y-jaw in the energy fluence of jaws together as a function of off-axis distance.

We notice from Fig. 3 that the fractional contribution of X-jaw is higher than Y-jaw. So, the X-jaw produces more secondary photons than Y-jaw. The position of jaw influences the characterizations of scattering photons on it. The secondary photons coming from X-jaw (near to the target) increases slightly with off-axis distance but the secondary photons coming from the Y-jaw (near to the phantom) decrease slightly too with off-axis distance and especially near to the beam edge region.

3.2. Energy fluence profile

The energy fluence profile describes the variation of the energy of photons as a function of off-axis distance. Fig. 4 shows the energy fluence profile of secondary photons emergent from X-jaw, Y-jaw, and jaws together.

The energy fluence profiles decrease with off-axis distance for all jaw components (jaws separately and together). The energy fluence of secondary photons originated in X-jaw is higher in comparison to Y-jaw. The secondary photons emergent from X-jaw are more energetic than the secondary photons emergent from Y-jaw. This difference due to the position of the jaws according to the target position.

Fig. 5 shows the fractional contribution of the energy fluence of X-jaw and Y-jaw in the energy fluence of jaws together as a function of off-axis distance.

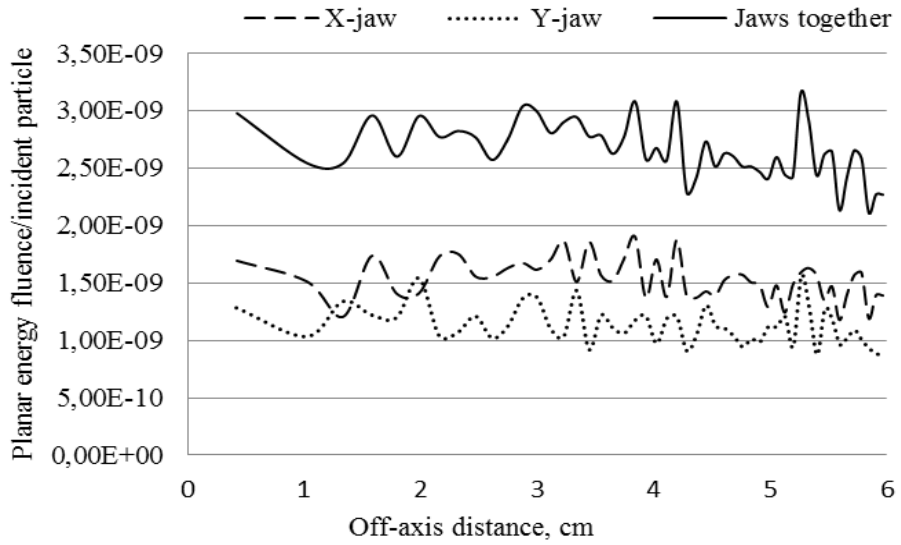

Fig. 4. Energy fluence profile of secondary photons originated in X-jaw, Y-jaw, and in jaws together as a function of off-axis distance.

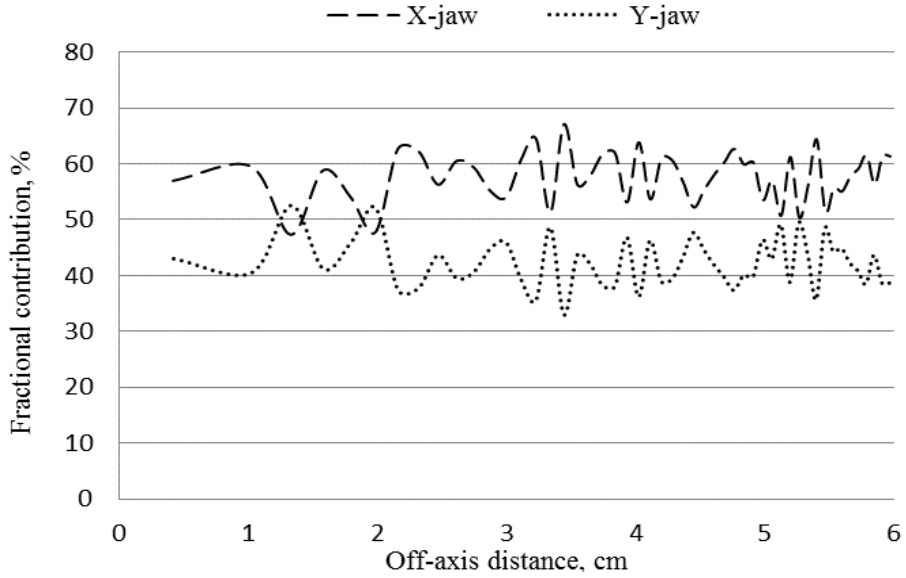

Fig. 5. Fractional contribution of the energy fluence of X-jaw and Y-jaw in energy fluence of jaws together as a function of off-axis distance.

It can be seen from Fig. 5, the energy fluence profile of secondary photons emergent from X-jaw increases slightly with off-axis distance, and the energy fluence of secondary photons emergent from Y-jaw decreases slightly with off-axis distance. The secondary photons of X-jaw are more energetic in comparison to the secondary photons of Y-jaw (Figs. 3 and 5)

3.3. Energy fluence distribution

The energy fluence distribution describes the variation of photon's energy as a function of energy. The energy fluence distributions are presented in Fig. 6 for secondary photons that originated in X-jaw and Y-jaw and jaws together.

All energy fluence distributions have a maximum of around 0.39 MeV that means the maximum number of secondary photons originated in jaws has approximately the energy of 0.4 MeV. The energy fluence profile of secondary photons emergent from X-jaw is greater than the energy fluence profile of secondary photons emergent from Y-jaw. For a good interpretation of these results, Fig. 7 presents the energy fluence distribution variation around the peak, which is presented in Fig. 6.

The maximum of energy fluence distribution of secondary photons emergent from X-jaw is 2.46 10^{-9} MeV/MeV/ incident particle at 0.49 MeV and the maximum of the energy of secondary photons emergent from Y-jaw is $1.89 \cdot 10^{-9}$ MeV/MeV/incident particle at 0.46 MeV. It can be seen that the energy fluence distribution of X-jaw is greater than Y-jaw.

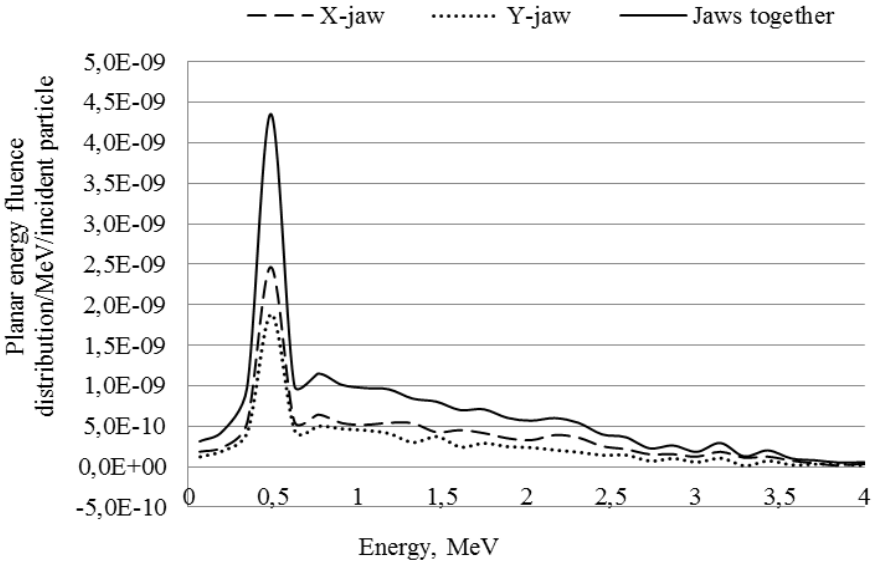

Fig. 6. Energy fluence distribution of secondary photons originated in X-jaw and Y-jaw and jaws together as a function of energy.

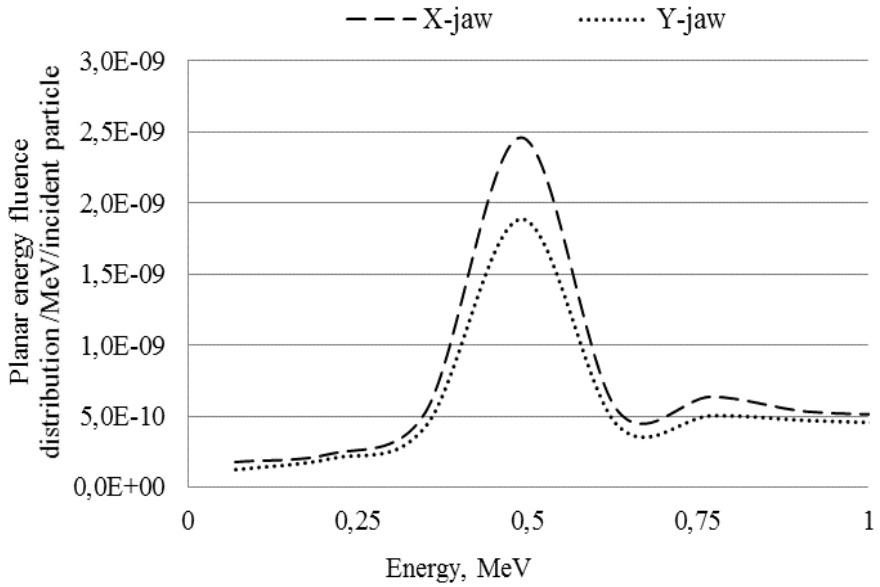

Fig. 7. Energy fluence distribution of secondary photons originated in X-jaw and Y-jaw as a function of energy.

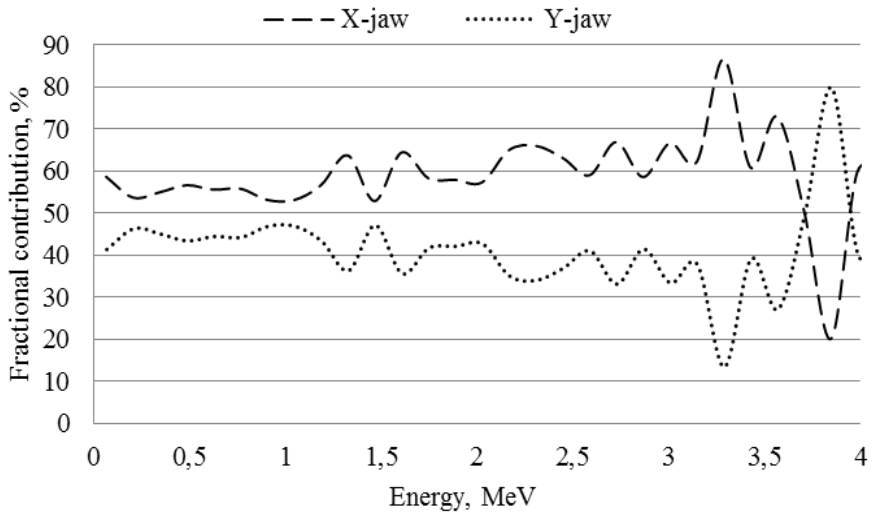

Fig. 8. Fractional contribution of energy fluence distribution of X-jaw and Y-jaw in energy fluence distribution of jaws together as a function of energy.

We notice from Fig. 8, the energy fluence distribution of secondary photons emergent from X-jaw increases with energy, and it is greater in comparison to energy fluence distribution of secondary photons emergent from Y-jaw. For energies more than 3.75 MeV, the fractional contribution values are caused by a low number of photons and the calculation fluctuation of Monte Carlo simulation and also to leakage photons in this region of the field [11].

The energy fluence distribution is significantly important for dose determination in the treatment planning system, the physicist should take into account the secondary photons dosimetry because they cannot reach the treatment volume, but they just penetrate the shallower depth and affect the healthy cells surrounding the tumor and the radiotherapy efficiency may be decreased.

3.4. Spectral distribution

Spectral distribution is the photon's number as a function of their energy. The knowledge of spectral distribution is crucial for the radiotherapy and radioprotection.

We notice from Fig. 9 that all spectral distributions have a maximum for secondary photons (X-jaw, Y-jaw, and jaws together) at the energy of 0.49 MeV, but they decrease for high energy. For good interpretation, Fig. 10 shows the spectral distribution around the maximum point for X-jaw and Y-jaw.

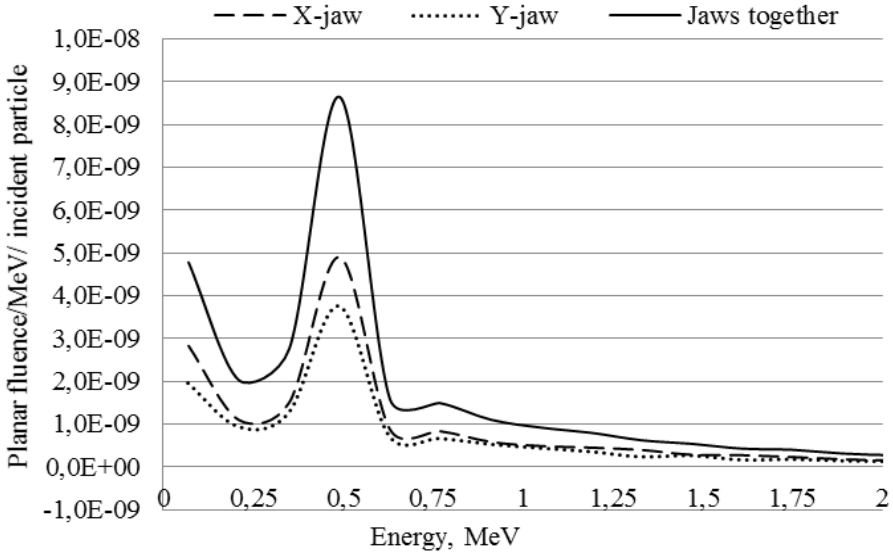

Fig. 9. Fluence of secondary photons originated in X-jaw and Y-jaw and jaws together as a function of energy.

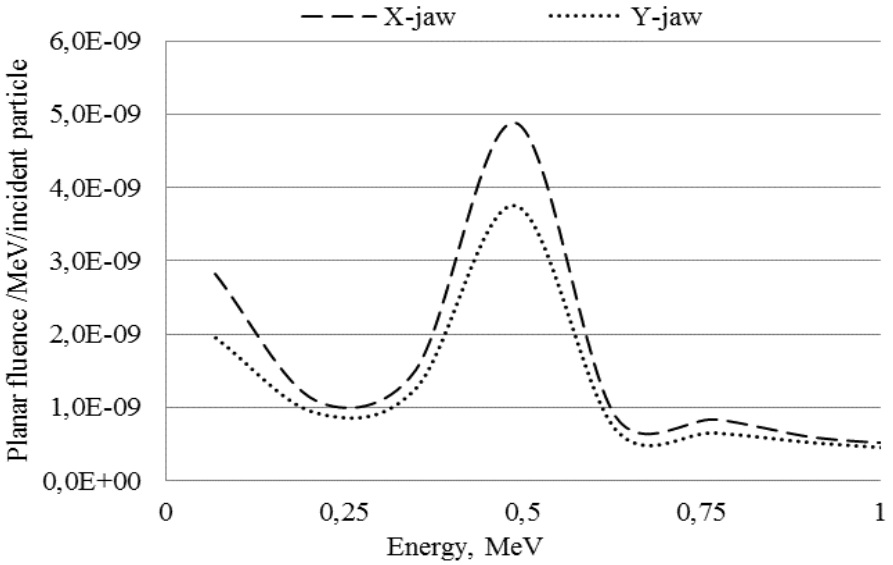

Fig. 10. Spectral distributions of secondary photons originated in X-jaw and Y-jaw as a function of off-axis distance.

We notice from Fig. 10 that there is a gap between the spectral distributions of X-jaw and Y-jaw and this gap is very large at the peak of the curves (0.49 MeV). For X-jaw, the spectral distribution maximum is $4.89 \cdot 10^{-9}$ photon/MeV/incident particle and for Y-jaw the maximum was $3.75 \cdot 10^{-9}$ photon/MeV/incident particle (see Fig. 10).

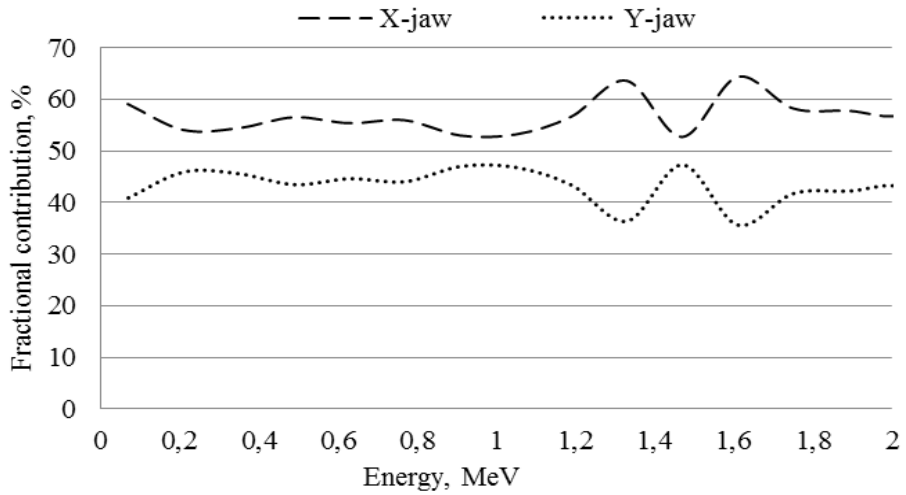

Fig. 11. Fractional contribution of the spectral distribution of X -jaw, and Y-jaw and in the spectral distribution of jaws together as a function of energy.

It can be seen from Fig. 11, the fractional contribution of the spectral distribution of secondary photons originated in X-jaw increases with energy and it is higher than the fractional contribution of the spectral distribution of secondary photons originated in Y-jaw and it decreases with energy. So, the position of jaws influences the spectral distribution of secondary photons emergent from each pear jaw (see Fig. 11). The fractional contribution values for energies more than 3.75 MeV are due to the low number of photons and calculation fluctuation.

3.5. Mean energy

The mean energy is evaluated the energetic behavior of the secondary photons emergent from jaws together and separately with off-axis distance. Fig. 12 shows the mean energy variation with off-axis distance.

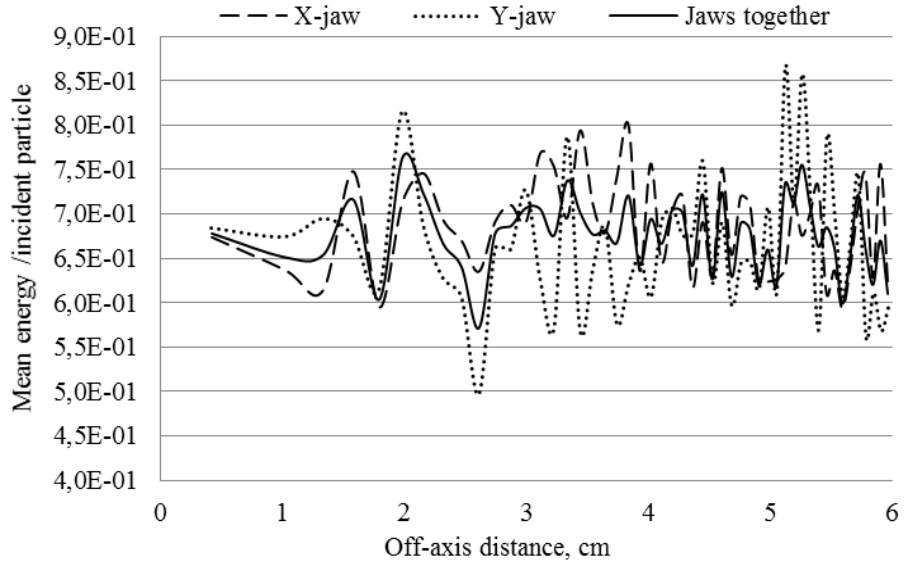

Fig. 12. Mean energy of secondary photons originated X-jaw and Y-jaw and in jaws together as a function of off-axis distance.

The mean energy of secondary photons originated in X-jaw is equivalent to the mean energy of secondary photons originated in Y-jaw, which means the position of jaws does not affect the mean energy of secondary photons originated in secondary collimators (see Fig. 12).

For more understanding, Fig. 13 shows the fractional contribution of the mean energy of each jaw in the mean energy of jaws together.

We notice from Fig. 13 that the position of jaws does not influence the mean energy of the secondary photons originated in the secondary collimators or jaws, the fractional contribution remains around 100 % for both jaws with a few fluctuations.

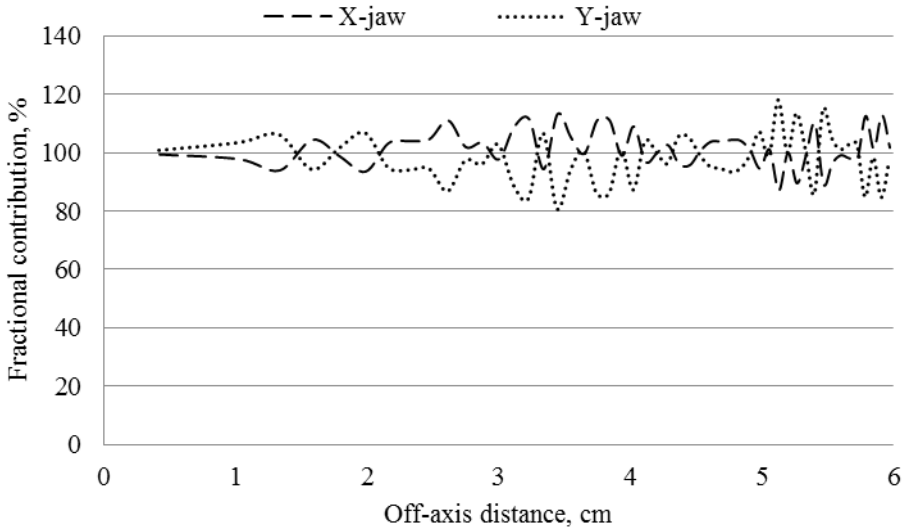

Fig. 13. Fractional contribution of mean energy of X-jaws and Y-jaws in the mean energy of jaws together as a function of off-axis distance.

3.6. Angular spread

Angular spread distribution characterizes the angle spread of photons after their interaction with jaws material. Fig. 14 shows the angular spread distribution of secondary photons originated in X-jaw and Y-jaw separately and jaws together.

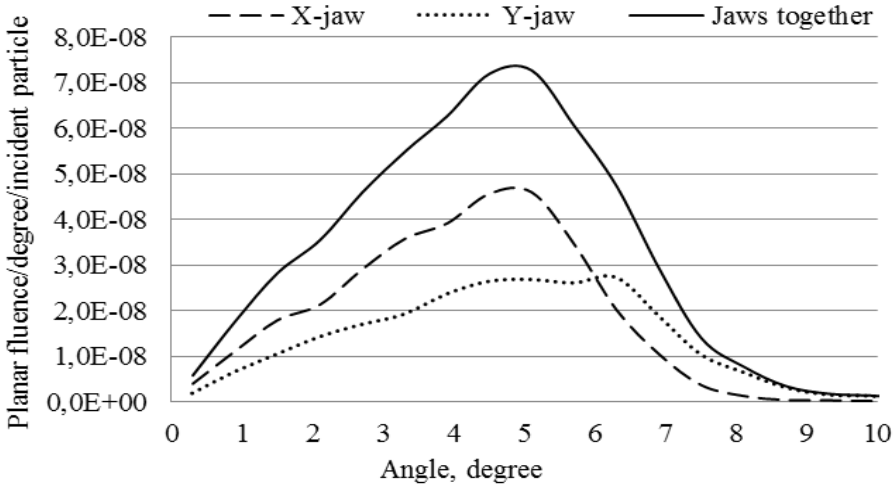

Fig. 14. Angular spread distribution of secondary photons of X-jaws, Y-jaws, and jaws together as a function of angular degree.

The angular spread distribution of secondary photons originated in X-jaw is higher than the angular spread distribution of Y-jaw. Angular spread distribution maximum for X-jaw is $4.59 \cdot 10^{-8}$ photon/degree/incident particle at 5.10° and angular spread distribution maximum for Y-jaw is $2.73 \cdot 10^{-8}$ photon/degree/incident particle at 6.30°. Therefore, the maximum of angular spread distribution decreases with jaws position on the beam central axis regarding the target, and the maximum position moves to the increasing angular degree (see Fig. 14).

For good interpretation of that result, Fig. 15 shows the fractional contribution of angular spread distribution of secondary photons originated in X-jaw and Y-jaw in angular spread distribution of secondary photons originated in jaws together.

We notice from Fig. 15, in the range of 0 to 6°, the angular spread distribution of secondary photons emergent from X-jaw is great and steady. It is more than 60 %. However, the angular spread distribution for Y-jaw is lower and also steady. It is less than 40 %. In the range of 6 to 10°, the angular spread distribution increases with the angle for the Y-jaw and reaches a maximum of 88 %, on the other side, it decreases with the angle for the X-jaw and reaches a minimum of 12 %.

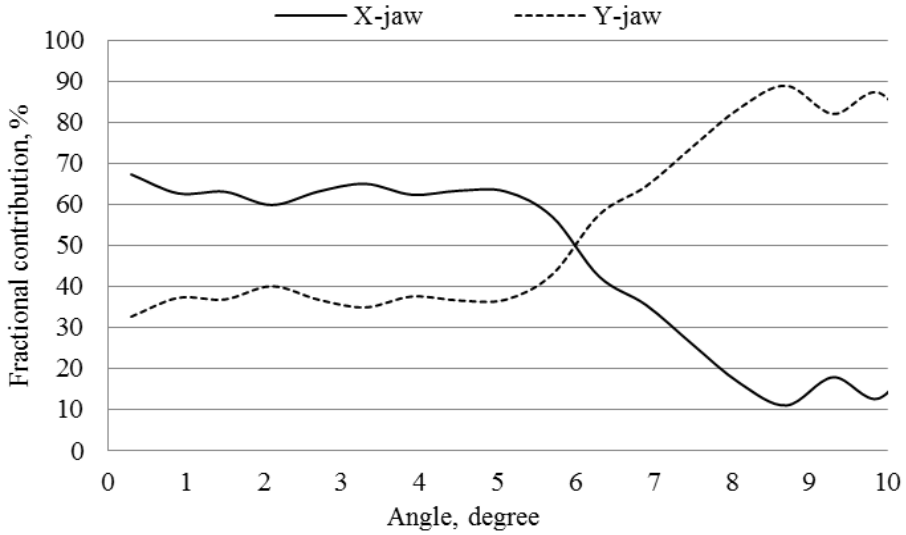

Fig. 15. Fractional contribution of angular spread distribution of X-jaw and Y-jaw in angular spread distribution of jaws together as a function of angle degree.

The angular spread distribution of secondary photons varies with the jaw position on the central beam axis regarding the target. This finding should be taken into consideration for radioprotection and radiotherapy treatment reasons.

4. Conclusion

Based on this study, the jaws can be potential sources of low energy photons and they might destroy the dosimetry quality of the produced photon beam (clinical beam) and subsequently the radiotherapy efficiency. The investigated photons are produced in high quantity and energy by X-jaw compared to Y-jaw. The position of jaws influences the scattering photons characterizations except for the mean energy which is approximately similar for both jaws.

Secondary photons originated in secondary collimator hurt the deep tumor treatment because they deposited their energy in the shallower depth and they could affect healthy tissues surrounding planning tumor volume. The International Atomic Energy Agency protocols recommend reducing the photons of low energy at the patient skin [12]. In light of these recommendations, we advise the physicists and physicians to take into account the secondary photons' effects in dosimetry determination according to the results of this work.

We would like to thank Varian Medical Systems for providing us the Varian Clinac 2100 geometry data and for the opportunity to study the Varian linear accelerator technology and take part in its future development.

REFERENCES

1. A.O. Ezzati et al. A comprehensive procedure for characterizing arbitrary azimuthally symmetric photon beams. Physica Medica 30(2) (2014) 191.
2. J.S. Cunha, D.N. Souza, A.B. Carvalho Junior. Dose calculation with MCNPX code for Total Body Irradiation technique in sitting and lying postures. Radiation Physics and Chemistry 149 (2018) 1.
3. J.P. Reis Junior et al. Simulation of Siemens ONCOR™ Expression linear accelerator using phase space in the MCNPX code. Progress in Nuclear Energy 70 (2014) 64.
4. M. Bencheikh, A. Maghnouj, T. Tajmouati. Photon beam softening coefficients evaluation for a 6 MV photon beam for an aluminum slab: Monte Carlo study using BEAMnrc code, DOSXYZnrc code and BEAMDP code. Moscow University Physics Bulletin 72(3) (2016) 263.
5. D.W.O. Rogers, B. Walters, I. Kawrakow. BEAMnrc Users Manual. NRCC Report PIRS-0509(A).
6. M. Bencheikh, A. Maghnouj, T. Tajmouati. Validation of Monte Carlo simulation of 6 MV photon beam produced by Varian Clinac 2100 linear accelerator using BEAMnrc code and DOSXYZnrc code. Phys. Part. Nucl. Lett. 14(5) (2017) 780.
7. D.W.O. Rogers et al. NRC User Codes for EGSnrc. NRCC Report PIRS-702.
8. M. Aljamal, A. Zakaria. Monte Carlo Modeling of a Siemens Primus 6 MeV Photon Beam Linear Accelerator. Australian Journal of Basic and Applied Sciences 7(10) (2013) 340.
9. C.M. Ma, D.W.O. Rogers. BEAMDP User's Manual. NRCC Report PIRS-0509(C).
10. P. Lonski et al. Assessment of leakage doses around the treatment heads of different linear accelerators. Radiation Protection Dosimetry 152(4) (2012) 304.
11. M. Bencheikh, A. Maghnouj, T. Tajmouati. Energetic properties' investigation of removing flattening filter at phantom surface: Monte Carlo study using BEAMnrc code, DOSXYZnrc code and BEAMDP code. Phys. Part. Nucl. Lett. 14(6) (2017) 921.
12. Absorbed dose determination in external beam radiotherapy. Technical Reports Series No. 398 (Vienna, International Atomic Energy Agency, 2000) p. 110.

М. Беншейх[1,*], А. Магхнудж[2], Д. Таджмуаті[2]

[1] Кафедра фізики, факультет наук і технологій Мохаммедія, університет Касабланки Хасана II, Мохаммедія, Марокко
[2] Лабораторія LISTA, кафедра фізики, науковий факультет Дхар Ель-Махраз, університет Сіді Мохамед Бен Абделлах, Фес, Марокко

*Відповідальний автор: bc.mohamed@gmail.com

АНАЛІЗ І ОЦІНКА ВТОРИННИХ ФОТОНІВ ВІД МОДИФІКАТОРА ПУЧКА ЧАСТИНОК ЯК РАДІАЦІЙНОГО ФОНУ НА ПОВЕРХНІ ФАНТОМУ

Дана робота зосереджена на вивченні геометрії та матеріалу модифікатора пучка частинок («щелеп»), що має вирішальне значення для покращення лінійного прискорювача за рахунок зменшення вторинних фотонів, що виходять з нього. Вони мають негативний вплив при лікуванні раку, особливо при пухлині, що глибоко розташована, оскільки їхня енергія виділяється на меншій глибині і може знищити здорові клітини, що оточують об'єкт лікування. Мета цієї роботи – дослідити та оцінити характеристики вторинних фотонів, що виникли у щелепах, з точки зору профілю потоку, розподілу енергії, спектрального та кутового розподілу. Ця робота була виконана за допомогою Монте-Карло кодів BEAMnrc та BEAMDP. Щелепи є потенційним джерелом вторинних фотонів, найближчим до фантома. Кількість вторинних фотонів, що виходять із X-щелепи (продовжня щелепа), є більшою, і вони більш енергійні порівняно із вторинними фотонами Y-щелепи (поперечна щелепа). Тому найбільш значущим результатом є отримання кутового розподілу вторинних фотонів для кожної пари щелеп. Для Y-щелепи більшість фотонів розсіюються з великими кутами, що означає, що ці фотони можуть вийти за межі поля опромінення і нанести шкоду здоровим клітинам, але для X-щелепи більшість вторинних фотонів знаходиться в полі опромінення; вони можуть впливати тільки головним чином на здорові клітини, що знаходяться перед об'єктом лікування.

Ключові слова: вторинний коліматор, Монте-Карло моделювання, вторинні фотони, код BEAMnrc, код BEAMDP.

М. Беншейх[1,*] А. Магхнудж[2], Д. Таджмуати[2]

[1] Кафедра физики, факультет наук и технологий Мохаммедия, университет Касабланки Хасана II, Мохаммедия, Марокко
[2] Лаборатория LISTA, кафедра физики, научный факультет Дхар Эль-Махраз, университет Сиди Мохамед Бен Абделла, Фес, Марокко

*Ответственный автор: bc.mohamed@gmail.com

АНАЛИЗ И ОЦЕНКА ВТОРИЧНЫХ ФОТОНОВ ОТ МОДИФИКАТОРА ПУЧКА ЧАСТИЦ КАК РАДИАЦИОННОГО ФОНА НА ПОВЕРХНОСТИ ФАНТОМА

Данная работа сосредоточена на изучении геометрии и материала модификатора пучка частиц («челюстей»), имеющих решающее значение для улучшения линейного ускорителя за счет уменьшения вторичных фотонов, выходящих из него. Они имеют негативное влияние при лечении рака, особенно при глубоко расположенной опухоли, поскольку их энергия выделяется на меньшей глубине и может уничтожить здоровые клетки, окружающие объект лечения. Цель этой работы - исследовать и оценить характеристики вторичных фотонов, возникших в челюстях, с точки зрения профиля потока, распределения энергии, спектрального и углового распределения. Эта работа была выполнена с помощью Монте-Карло кодов BEAMnrc и BEAMDP. Челюсти являются потенциальным источником вторичных фотонов, ближайшим к фантому. Количество вторичных фотонов, выходящих из X-челюсти (продольная челюсть), больше, и они более энергичны по сравнению с вторичными фотонами Y-челюсти (поперечная челюсть). Поэтому наиболее значимым результатом является получение углового распределения вторичных фотонов для каждой пары челюстей. Для Y-челюсти большинство фотонов рассеиваются с большими углами, что означает, что эти фотоны могут выйти за пределы поля облучения и нанести вред здоровым клеткам, но для X-челюсти большинство вторичных фотонов находится в поле облучения; они могут влиять только главным образом на здоровые клетки, которые находятся перед объектом лечения.

Ключевые слова: вторичный коллиматор, Монте-Карло моделирование, вторичные фотоны, код BEAMnrc, код BEAMDP.

Надійшла/Received 21.01.2019